Chinese Society of Aeronautics and Astronautics
& Beihang University

Chinese Journal of Aeronautics

cja@buaa.edu.cn
www.sciencedirect.com

REVIEW ARTICLE

Advances and trends in plastic forming technologies for welded tubes

Zhan Mei [*], Guo Kun, Yang He [*]

State Key Laboratory of Solidification Processing, School of Materials Science and Engineering,
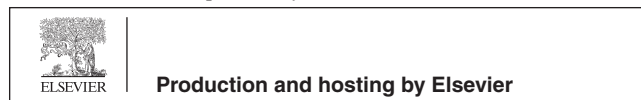Northwestern Polytechnical University, Xi'an 710072, China

Abstract With the implementation of environmental protection, sustainable development and conservation-oriented policies, components and parts of thin-walled welded tubes have gained increasing application in the aircraft and automotive industries because of their advantages: easily achieving forming and manufacturing process at low cost and in a short time. The current research on welded tube plastic forming is mainly concentrated on tube internal high-pressure forming, tube bending forming, and tube spinning forming. The focuses are on the material properties and characterization of welded tubes, finite element modeling for welded tube forming, and inhomogeneous deformation behavior and the mechanism and rules of deformation coordination in welded tube plastic forming. This paper summarizes the research progress in welded tube plastic forming from these aspects. Finally, with a focus on the urgent demand of the aviation, aerospace and automotive industries for high-strength and light-weight tubes, this paper discusses the development trends and challenges in the theory and technology of welded tube plastic forming in the future. Among them, laser tailor-welded technology will find application in the manufacture of high-strength steel tubes. Tube-end forming technology, such as tube flaring and flanging technology, will expand its application in welded tubes. Therefore, future studies will focus on the FE modeling regarding how to consider effects of welding on residual stresses, welding distortions and microstructure, the inhomogeneous deformation and coordination mechanism of the plastic forming process of tailor-welded tubes, and some end-forming processes of welded tubes, and more comprehensive research on the forming mechanism and limit of welded tubes.

[*] Corresponding authors. Tel.: +86 29 88460212 805 (M. Zhan), +86 29 88495632 (H. Yang).
E-mail addresses: zhanmei@nwpu.edu.cn (M. Zhan), gkyike@163.com (K. Guo), yanghe@nwpu.edu.cn (H. Yang).
Peer review under responsibility of Editorial Committee of CJA.

Production and hosting by Elsevier

1. Introduction

Compared with seamless tubes, welded tubes have advantages, such as low production cost, high production efficiency, stable quality and variety, etc. With the implementation of environmental protection, sustainable development and

conservation-oriented policies and the rapid development of lightweight structure forming manufacturing technology in the aviation, aerospace and automotive industry, all types of thin-wall welded tube parts and components are finding increasingly extensive application.[1–4] Especially in the aviation industry, the tubing system is the core part of the aircraft. Because of high material utilization rate, high production efficiency, and the properties of expanding and bending forming having little difference with seamless tube, welded tube is finding wide application in aircraft environmental control and drain line system. From the perspective of plastic forming, welded tube plastic forming belongs to the category of inhomogeneous materials forming. The welded tube forming process is similar to that of homogeneous tubes with wrinkling, cracking and other possible defects, while inhomogeneous materials and the performance of the parent metal, the weld seam (weld line or weld bead) and the heat-affected zone (HAZ) of welded tubes lead to a complicated nonlinear materials problem. The width of the weld seam and the HAZ and their positions in the plastic forming process will result in a complicated geometrical nonlinear problem. Material and performance differences among the weld seam, the HAZ and the parent metal in the plastic forming process may also lead to a complex contact with the tool and die and boundary nonlinear conditions. These nonlinear problems and their coupling effects enhance the restriction of the weld (including the weld seam and the HAZ) on the plastic forming quality of welded tubes and make the plastic forming quality and forming performance/forming limit of welded tubes more sensitive to the rules of constraints and deformation coordination among the weld seam, the HAZ and the parent metal. When the effect of inhomogeneous deformation among these zones is so strong that they cannot deform in a coordinated fashion, defects such as wrinkling and fracture may occur. Furthermore, these defects will constrain the normal plastic forming process of welded tubes and the improvement in their forming performance. When each zone of the welded tubes can be deformed in a coordinated fashion, it is likely that the plastic forming process can be carried out smoothly, thereby improving the forming quality of the welded tubes and fully exploiting the tubes' deformation potential and improving their forming performance. These characteristics make the plastic forming behavior of welded tubes different from those of homogeneous tubes. Therefore, it is important to perform research on welded tube plastic forming theory and technology. This research will provide a practical engineering theory basis for improving the quality of plastic forming of welded tubes and for exploring the deformation potential of these tubes. It is significant and important for improving the level and capability of the high-quality, low-cost, and short-cycle manufacturing technology of welded tubes.

To date, the welded tube plastic forming research mainly concentrates on three aspects, including internal high pressure forming, bending forming and spinning forming. The focus is on material properties and the characterization of welded tubes, finite element modeling for welded tube forming, and inhomogeneous deformation behavior in welded tube plastic forming and the mechanism and rules of deformation coordination. Based on these aspects, this paper summarizes the research progress in welded tube plastic forming.

2. Material properties and constitutive modeling of welded tubes

Different welding technologies and processes will produce weld seams and HAZs with different appearances, sizes and mechanical properties. This has a significant effect on the forming performance. Therefore, it is necessary to perform research on welded tube performance and its characterization.

2.1. Weld characteristics of welded tubes

The appearance, size, mechanical properties and plastic forming performance of the weld line and the HAZ are closely related to the welding process, the speed, the temperature, the extrusion force and the thickness of the tube. Through metallographic analysis and tensile testing, Chen[5] investigated the mechanical non-uniformity of a 304 (SUS304) austenitic stainless steel welded joint of tailor-welded tubes that were made using tungsten inert gas (TIG) welding technology. He analyzed the variations and differences in the microstructure and mechanical properties of different zones of welded joints and ascertained that the width of the weld was approximately 5 mm, and divided the welded joints into four regions, including parent metal, HAZ, fusion zone (or in some cases only a fusion line) and weld seam. Khalfallah[6] ascertained that the weld seam width of a low-carbon steel S235JR tube welded by high-frequency induction welding was approximately 1 mm and that the width of each HAZ was approximately 2 mm. The weld region in their study was characterized by much higher hardness (approximately HV = 198) than that of the parent metal (approximately HV = 115). The yield and tensile strength stresses of the weld specimen were higher than those of the parent metal, whereas the strain hardening exponent and the uniform elongation were lower for specimens containing the weld than those of the parent metal.[6] Ghoo et al.[7] and Panda et al.[8] also obtained similar findings. Yang et al.[9] ascertained that the weld width of a QSTE340 welded tube produced by resistance welding was 4 mm and the width of each HAZ was 6 mm by analyzing the weld joint microstructure and microhardness distribution. For high-frequency electric resistance welding (HF-ERW)[10] and extrusion welding[11], the weld is always funnel-form. Ren et al.[12] observed the weld shape to be like a typical drum by means of microhardness distribution and microstructure analysis. They found that the difference among the parent material, the HAZ and the fusion zone was apparent and determined that the weld seam width of 60 mm × 4.0 mm ($d \times t$:d-tube outside diameter, t-wall thickness) and 78 mm × 2.7 mm QSTE340 HF ERW tubes were both 0.4 mm and the width of the HAZ of both tubes was 2.4 mm. Li et al.[13] used tensile tests and microhardness tests to study the mechanical performance of a CP3 pure titanium thin-walled welded tube which would be used in the drain line system of a civil aircraft. Their results show that compared with the parent metal, the yield strength and tensile strength of the weld were higher, but the elongation of the weld was obviously lower, and a large hardness gradient appeared in the HAZ. Ren[14] also obtained similar conclusions in the research on QSTE340 steel welded tubes. A large number of studies show that welding caused a change in the hardness of the weld area. For example, in laser welding, the weld area hardness increased by 50%[15] to

250%[16]. In most cases, the weld hardness increased by approximately 120%[17].

2.2. Material modeling of welded tubes

The material properties of the weld seam and the HAZ have a close relationship with the constitutive model of welded tubes. Therefore, accurate constitutive modeling of the welding seam and HAZ is necessary for evaluating the welded tubes' plastic formability through theory and finite element analysis (FEA). There are four main methods for determining the material properties and constitutive relationship of the weld seam and the HAZ of welded tubes.

The first method is to obtain the material properties of the weld seam and the HAZ through uniaxial tensile testing of standard specimen or non-standard small specimens made only of the weld seam and the HAZ[18,19]. In this method, the results obtained from using a non-standard specimen are different from those using a standard specimen. This is because as the specimen size increases, the resistance tensile stress of the weld is weakened; thus, the material properties of the weld and the HAZ are particularly sensitive to the specimen size[20]. When the relative size of the weld on the specimen cross section increases, the stress–strain curve of the specimen tends to be closer to the stress–strain curve of the weld seam, so many researchers choose to use small specimens or microspecimens to determine the material properties of weld tubes[21,22]. However, it is difficult to cut the specimen which contains only the weld or the HAZ because of the narrow width of the welding seam and the HAZ and their irregular cross sectional shape. Davies et al.[23] showed that the plastic deformation ability of the tensile specimen decreases as the proportion of the weld in the cross section of the specimen increases by tensile testing different sizes of samples. This means that the results obtained by this method have a great degree of dispersion.

The second method is to use an empirical formula based on microhardness; i.e., the material properties of the weld and the HAZ are determined according to the microhardness distribution of the weld and its surrounding area, and, using the directly proportional relationship between the flow stress and microhardness, the material properties of the weld and HAZ are determined.[24] The microhardness method is simple, convenient, and fast; it does not cause damage to the specimen. And this method is often used for obtaining weld joint material properties. However, this method neglects the effect of the welding method and welding parameters on the weld properties, and there is no mature hardness criterion for the width of the weld seam and HAZ.

The third method is commonly used in obtaining the weld joint material properties and constitutive relationship based on the rule of mixtures.[25–27] This method uses a mixture of tensile specimens that include the weld and the surrounding material. Then, based on the strain mixture rule of the weld seam, the parent metal and the HAZ, the constitutive relation of the weld and HAZ can be determined. This method is an indirect method for obtaining the characteristics of the weld material, avoiding the disadvantages of the first method. When adopting the rule of mixtures to confirm the plastic constitutive relationship of the weld material, the cross-sectional size must be accurately determined. Because there are no distinct boundaries among the weld bead, the HAZ and the parent metal in the macrostructure, it is difficult to distinguish between them.[20] Furthermore, during the preparation of the mixed specimen according to the standard sample requirements, it is inevitable that some HAZ and parent metal will be included in the mixed specimen. Thus, the properties determined from the tensile test of the mixed specimen are not only those of the weld seam and HAZ but also partly those of the parent metal. In view of the above shortcomings, Zhan et al.[20] proposed a microhardness measurement method using cross-sectional samples of the tube to truly represent the microhardness distribution characteristics along the thickness direction throughout the weld zone, HAZ and parent metal. They also proposed a new method for establishing the constitutive relation of inhomogeneous materials based on the rule of mixtures and subdividing the HAZ into strips. This modified rule of mixtures diminished the effects of the width of a mixed specimen on the flow stress–strain to some degree, and it could accurately and continuously reveal the variation in flow stress across the HAZ. Using this method, a more precise constitutive model of a Q215 welded tube was obtained by Zhan et al.[20] Using this method, Ren et al.[28] established a high-precision material constitutive model of a QSTE340 welded tube.

The fourth method is the digital image correlation (DIC) method. This method was initially proposed by Reynolds and Duvall[29] based on the iso-stress load assumption. It is easy to capture strain distributions in the local area near the weld line and in the whole deformation area using DIC.[30,31] Since then, this method has been frequently used for characterization of the mechanical properties of friction stir welds (FSW)[32–37] and laser welds.[38,39] Louëdec et al.[40] proposed an inverse procedure based on DIC and the virtual fields method to accurately identify the evolution of the mechanical properties throughout the weld. They applied the method to determine the local elasto-plastic properties of an Al 5456 FSW weld. Their results indicated that the plastic parameters in the center of the weld underwent a significant change even at a low strain rate. Two-dimensional (2D) DIC can only measure the surface displacement of the object surface. To solve the error caused by the displacement of the plane in the process of the 2D correlation operation, Chao et al.[41] realized the three-dimensional (3D) displacement measurement of the curved surface by combining computer vision theory and the 2D digital image speckle technique. Li et al.[42] proposed an identification method for the mechanical properties of the weld and HAZ by combining the 3D DIC technique with a genetic algorithm (GA)-driven inverse approach. They applied the method to dual-phase high-strength steels (DP600 and DP980) with a thickness of 2 mm. Dick and Korkolis[43] used 3D DIC technology to probe the full strain fields during the Ring Hoop Tension Test (RHTT) of an extruded Al-6061-T4 tube. By coupling this information with extensive FEA, they decoupled the effects of the tube wall thickness eccentricity, tube-mandrel friction and specimen preparation from the recorded response. Fu et al.[44] proposed a refined method for identifying the material parameters of a weld line based on the DIC technique and the hardness test. The material parameters of the power exponent material hardening model of the weld zone and two HAZs were obtained indirectly by the DIC technique and the hardness test. Their comparison of FEA and experiments shows that the refined method was better than the traditional method. Chen and Lin [45] proposed a performance parameter

identification partition allocation method of a tailor-welded blank (TWB) based on the DIC technique. In this method, the weld was divided into the weld seam and the HAZ, the performance of the HAZ was regarded as continuously varying, and a calculation model of the weld performance parameters was established.

2.3. Existing problems and development directions

An in-depth study of inhomogeneous deformation behaviors of the weld seam, HAZ and parent metal of welded tubes and their plastic forming properties in the plastic forming process requires a constitutive model that can accurately describe material plastic flow and deformation behavior. However, due to the non-uniformity in the materials of welded tubes, narrow weld seams and HAZ widths and their complicated shape, it is difficult to directly capture tensile samples of the weld and HAZ to obtain its material property parameters and constitutive model. Therefore, at present, the most widely established constitutive model of welded tubes is the rule of mixtures and its improvement. However, even though by using the improved rule of mixtures method the material properties across the weld seam and HAZ can be obtained by subdividing the HAZ, and it is still difficult to identify the material properties across the weld seam and HAZ with a smooth transition. Therefore, because of the superiority of DIC technology, which is a non-contact and whole field measurement, a growing number of studies choose the DIC method to determine the material properties of welded tubes and to establish their constitutive model. The accuracy of DIC technology is mainly influenced by the load system, the imaging system and the correlation algorithm; therefore, how to select the appropriate algorithm is the primary problem for the application of DIC technology in the stress–strain measurement of welded tubes. Meanwhile, due to the complex inhomogeneous material properties in the weld, the HAZ and the parent metal, developments are under way to establish a more accurate constitutive model combining DIC with other methods and considering the characteristics of welded tubes.

3. Weld characterization in FE modeling

In recent years, the finite element method has been widely used in the studies of welded tube plastic forming. This research mainly focuses on establishing the corresponding finite element models of internal high-pressure forming, numerical control (NC) bending, and spinning forming of welded tubes. However, the differing appearances, sizes and mechanical properties of the welds and the HAZs resulting from different welding processes increase the complexity of the finite element modeling of welded tube plastic forming process.

3.1. FE modeling for welded tubes

According to the treatment methods for the weld seam and the HAZ, the finite element models for welded tubes can be classified into the following four categories.

The first category can be called the pure parent metal FE model. As shown in Fig. 1(a), the model neglects the weld and the HAZ, and the whole tube is regarded as a homogeneous tube endowed with the material properties of the parent metal.[3] This simplified modeling method will result in incorrect results in some cases.[46] Kim et al.[3] established a finite element model of the welded tube free-bulging process without considering the weld and the HAZ. The simulation results show that the fracture integral value along the middle tube ring changed little. Therefore, it was difficult to predict the fracture failure location of the welded tube free-bulging process.

The second category is the FE model that includes both the parent metal and the weld. As shown in Fig. 1(b), this model only considers the effect of the weld material properties and ignores the existence of the HAZ.[3] There are three methods for establishing the model of the weld seam.[47–55] In the first method, solid elements based on the size, shape and material parameters of the weld are adopted to establish accurately the model of the weld. In the second method, shell elements are used to establish a model of the weld. In the third method, changes in the weld material properties are ignored, and considering only the weld position, the weld is replaced by a row of beam elements or shell mesh elements or the weld is treated as a rigid pivot. Zhao et al.[48] described the weld using a rigid pivot, a shell element and a solid element. Comparison of the simulation results of these models for a free-bend test, stretch-bend test and limited dome-height test with experimental results show that the simulation accuracy was the lowest when the weld was simplified to a rigid pivot, and the accuracy was quite similar when the weld was simplified to shell elements and solid elements. In general, although the FE model,
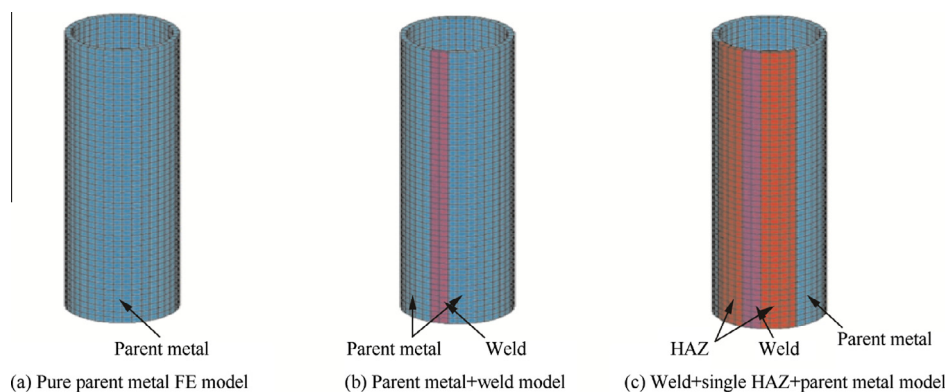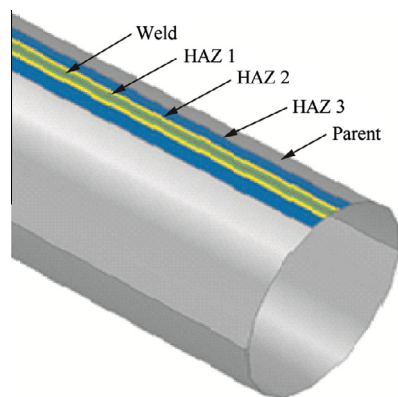

(a) Pure parent metal FE model   (b) Parent metal+weld model   (c) Weld+single HAZ+parent metal model

Fig. 1   Finite element models of welded tubes.[3]

including both the parent metal and the weld, is closer to the actual situation than the pure parent metal model, it can still cannot accurately predict the wall thickness variation, rupture and failure of the HAZ in the plastic forming process,[56] while the HAZ is always a high-failure area with low strength, poor plasticity and many inclusions and other defects.

The third category is the model that includes the weld, a single HAZ and the parent metal. As shown in Fig. 1(c), in this model, the differences of the material properties of the weld seam, the HAZ and the parent metal are considered.[3] Compared with the previous two models, this method can accurately simulate the deformation characteristics of the weld joint plastic forming. Kim et al.[3] created three finite element models for the parent metal alone (Model A), for including the weld and the HAZ as well (Model B), and for including the weld only (Model C) to numerically predict bursting failure during the bulging process of a seamed tube. The results show that for model B, the maximum value of the potential initial fracture site occurred near the weld line, which coincided with one of the actual bulging tests. Therefore, the finite element model containing the weld and the HAZ was the best model among the three models in describing the bursting behavior numerically. Rogue et al.[57] created two models of a welded-tailor tube, with and without a HAZ, to compare different approaches to modeling of the HAZ. They show that the results were clearly influenced by the presence of the HAZ and that by increasing the difference between thicknesses, the presence of a well-defined HAZ could have greater influence on the final results.

The fourth category has an FE model that includes the weld, the subdivided HAZs and the parent material (see Fig. 2). This model considers not only the differences in the material properties between the weld and the HAZ but also the gradual change in the material properties of the HAZ.[28] Using this method, Galdos and Garcia[56] subdivided the weld and HAZ into seven subzones. Their simulation results show that the thickness distribution of the weld and the HAZ were consistent with the experimental results. Liu et al.[58] studied an FE simulation of NC bending of 60 mm × 4 mm welded tubes. They showed that the results obtained by the simulation of the subdivided HAZ model were closer to the experimental results. Ren et al.[28] established an FE model including the weld, a subdivided HAZ and the parent material that considered the varied material properties of each HAZ for the NC

Fig. 2 Weld + subdivided HAZ + parent metal FE model[28] for welded tubes.

bending process of 78 mm × 2.7 mm QSTE340 welded tubes. As shown in Fig. 2, each HAZ of the welded tube was subdivided into three subzones in this model.

3.2. Existing problems and development directions

To sum up, establishing FE models of welded tubes containing the weld seam, a subdivided HAZ and the parent material considering the varying material properties of the weld, the HAZ and the parent metal for plastic forming of welded tubes has become a trend. For the model elements, the accuracy and the efficiency should be considered comprehensively according to the actual tube size and the weld characteristics.

The mechanical properties of the welded joints are smooth and continuous along the vertical direction of the weld; while in the solid FE model, this complex continuity problem in these domains is discretized by using mesh partitions.[59] Because the widths of the weld line and the HAZ are much narrower than those of the parent zone, the mesh in the weld line and HAZ have to be much finer than that of the parent zone to approach the continuity by establishing an FE model with the weld and subdivided HAZs. This model can improve the simulation accuracy, on the one hand; however, in contrast, the calculation efficiency is low. The FE model simplifying the weld with a row of beam elements, shell element mesh, or a rigid hinge link has high computational efficiency but low accuracy because it only considers the effect of the weld position and ignores the variation in material properties in the weld, HAZ and parent zones.

Therefore, how to establish an accurate and efficient FE model for welded tube plastic forming considering the variation in material properties across the weld seam, the HAZ and the parent zone becomes a key problem at present. The main difficulty in the process is how to model the weld seam and HAZ as accurately as possible to improve the computational accuracy on the one hand and how to improve the calculation efficiency on the other hand.

As we all know, welding process also brings about residual stresses as well as welding distortions and micro-structural transformation. Even heat treatment after welding can reduce or remove residual stresses, it will result in variation on tube geometry and microstructure. However, there is no research on FE modeling considering all these effects from welding and heat treating except for some analyses on residual stress of tubes after welding[60–63]. Therefore, a macro–micro coupled FE modeling for the complete process chain including welding, heat treating, followed by the particular plastic forming is needed to accurately simulate welded tube plastic forming process.

4. Constraining effect and deformation coordination in welded tube plastic forming

Due to that the material properties are different in different zones of welded tubes, inhomogeneous plastic deformation and mutual restriction exist in the plastic forming process of welded tubes. When the effect of inhomogeneous deformation between each zone is prominent, they are incapable of deforming in coordination; thus, defects, such as rupture, emerge that constrain the normal process of welded tube plastic forming and the improvement of forming quality and forming limit.

Therefore, inhomogeneous deformation and coordination among the weld, the HAZ and the parent metal will have an important influence on the plastic forming behavior and forming limit of welded tubes.

4.1. Constraining effect and deformation coordination

Except for the inhomogeneous plastic deformation and coordination in the outside and inside deformation zones of seamless tubes,[64] there also exist the inhomogeneous plastic deformation and coordination in the parent metal, HAZ and weld zones of welded tubes. The inhomogeneous plastic deformation and coordination of welded tubes were studied by many scholars whose major in researching NC bending, hydroforming and spinning.

For the NC bending process of welded tubes (see Fig. 3), Ren[14] proposed a constraining factor that considered the geometrical characteristics and materials heterogeneity of the weld and HAZ in investigating the influence of geometrical characteristics and material heterogeneity of the weld region on the constraining effect and deformation coordination of welded tubes. By this constraint factor, Ren et al.[28] revealed the constraining effect of the weld and HAZ and their positions (see Fig. 4) on the QSTE340 welded tubes in NC bending forming and the deformation coordination laws in different areas. They found that the larger the constraining factor of the weld region is, the larger the constraining effect of the weld on the tube bend formability is. They also found that the constraining effect caused by the weld increased the cross-sectional deformation and the hoop strain in the weld region, decreased the

thickness strain compared with the homogeneous tube, and had little effect on the springback angle. Li et al.[13] analyzed the effect on wall thinning and cross section flattening of the NC bending of a CP3 pure titanium welded tube. They found that the wall thinning of the weld region was less than that of homogeneous tubes and that the weld seam only had a significant effect on the wall thinning of the material near the tube-clamping end. Liu et al.[59,65] found that the weld and HAZ had a great influence on the stress across the weld but little influence on the strain distribution of an HFRW QSTE340 welded tube and proposed a concept of weld relative strength factor S_f; then, they studied the influence of S_f on the wrinkling and wall thickness distribution of welded tubes. Their results showed that the S_f had the most significant influence on the degree of wall thinning when the change in S_f was caused by the weld anisotropy exponent. The ratio of the degree of wall thinning was reduced greatly (approximately 37.61%), when S_f increased slightly (approximately 0.89%). Ren[14] revealed the effect of forming parameters, such as the clearance between the tube and the die, and the push assistant lever and the number of balls, on the 78 mm × 2.7 mm × 156 mm QSTE340 welded tubes bend formability and deformation coordination. The results show that the larger the clearance is between the tube and the wiper die or between the tube and the mandrel dies, the larger is the friction on the tube-pressure die; additionally, the smaller the clearance is between the tube and the pressure die, the smaller is the friction on the tube-wiper die.

In the hydroforming of welded tubes, Aue-U-Lan et al.[66], Sun and Yang[67,68] found that inhomogeneous deformation had an influence on the material flow of the weld, which resulted in inhomogeneous distribution of the wall thickness and asymmetric shape of the welded tubes. Liu et al.[69] investigated the ratio of the maximum bulging amount of a thick tube and the limit bulging amount of a thin tube to scale deformation coordination of tailor-welded tube hydroforming. Their results show that with increasing length ratio and thickness ratio, the deformation coordination was obviously improved. Chu et al.[70,71] revealed the deformation behavior and the weld seam movement of tailor-welded tubes during hydroforming, the initiation and expanding of the plastic deformation and the factors that affect hydroforming together by using FEA and experiments. Their results show that different strain states during the bulging process were the intrinsic feature of weld seam movement, and the deformation coordination could be
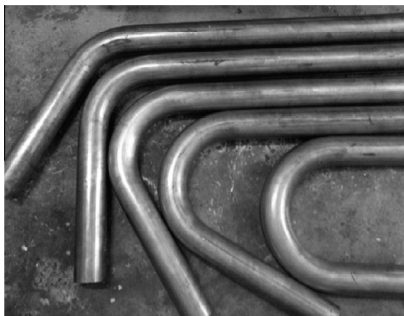

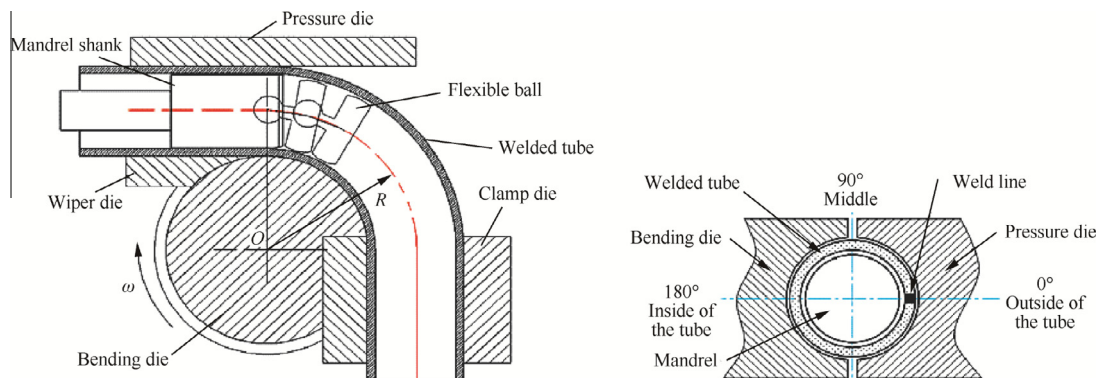**Fig. 3**   Production of bending forming of welded tubes.[28]

Fig. 4   Schematic diagrams of welded tube NC bending process and weld position.[28]

improved by increasing the hardening exponent and the length ratio. As shown in Fig. 5, Imaninejad et al.[72] conducted tube hydroforming experiments and FEA to develop the forming limit diagram of AA6082-T4 by utilizing three types of end-conditions. It was found that "free-end" hydroforming gave the lowest forming limits, followed by "pinched-end" and "forced-end" hydroforming, and the anisotropy of the weld material and the end-condition used during hydroforming experiments had the largest influence on the failure location with respect to the weld center.

In the deformation behavior of welded tube spinning forming (see Fig. 6), Yuan et al. [73] found that the spinning increased the formability of 2024-O aluminum alloy FSW joints significantly. Their results show significant improvement in the uniformity of the microhardness distribution and the tensile and yield strengths of FSW joints. Moreover, they revealed that the strengthening mechanism of the tube was that spinning not only refined grain but also broke the second phase and increased the density of the dislocation. Wang et al.[74] studied the influence of spinning on the formability of 2024-O aluminum alloy FSW tubes by the hydraulic bulge test and reached conclusions similar to those of Yuan et al.[73] They revealed the difference in grain size and precipitates between the weld and the parent metal, leading to an asymmetric W-type microhardness distribution after spinning. When compared with the result of tensile tests, the tube after spinning showed better formability when the stress state changed from a uniaxial to a biaxial stress state. Zhang et al.[75] obtained an ultra-thin-wall cylinder with a radius of 558 mm and a wall thickness ratio of 0.42 mm by deeply cold spinning on a C-276 nickel-based alloy welded cylinder and analyzed the effect of deeply cold spinning on the mechanical properties, microstructure and corrosion resistance of the parent metal and the weld. Their results show that the grains in the parent metal were obviously refined, that the orientation of the grains was enhanced after cold spinning with a thickness reduction of 80% and that the grains in the weld seam were transformed from coarse and long fishbone dendrites into small granular grains.

4.2. Forming limit of welded tubes

In the plastic forming process of welded tubes, due to the complex material, geometrical nonlinearity and the coupling effect between them, the welded tubes often incur defects, such as cracking and wrinkling. To date, researchers have paid much more attention to the forming limit of welded tubes in hydroforming and bending processes.

Ma et al.[77] developed a measurement method for the limit strain at the tension–tension strain zone of a forming limit diagram (FLD) based on a tube ellipse bulging test. They generated the FLD of HR340 laser-welded tubes in different sizes. Their results show that the thickness and diameter of welded tubes made from the same brand of sheet material not only affected the limit strain in the plane strain state but also affected the shape of the forming limit curve (FLC). Chen et al.[78] developed a novel theoretical method to predict the FLD for welded tube hydroforming, considering the unique features of seamed tube hydroforming. Based on this theoretical method, they proposed a new prediction model for the forming limit of welded tube hydroforming using the Swift hardening equation and the Hill yield criterion. Based on this prediction model, they calculated the FLD for ERW QSTE340 welded tubes. Their results show that the forming performance of the welded tubes was obviously inferior to that of the parent metal blank, so the hydroforming FLC of the welded tubes could not be replaced by the FLC of the welded blank.

However, in the above methods the influence of the weld seam and the HAZ on the forming limit of the welded pipe is not considered. By using the FEM combined with Oyane's ductile fracture criterion, Kim et al.[3] investigated the forming limit and bursting pressure level for a seamed tube. Through a series of FEAs they found that the initial fracture took place in the HAZ near the weld line. Considering that the over-thinning resulting from local necking was the dominant failure for the welded tube with high strength and a small bending radius and wall thickness, Ren[14] proposed a method for determining the forming limit of welded tube bending (the minimum bending radius) dependent on admitted thickness
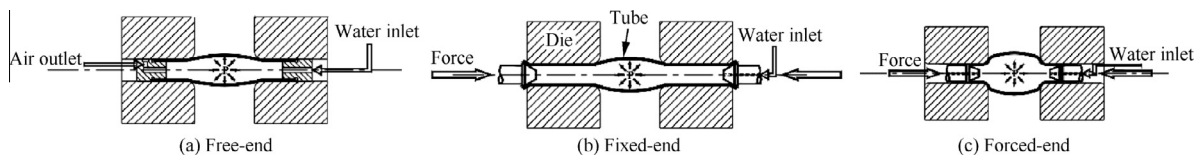

Fig. 5   Schematic illustration of end-conditions used during hydroforming.[72]
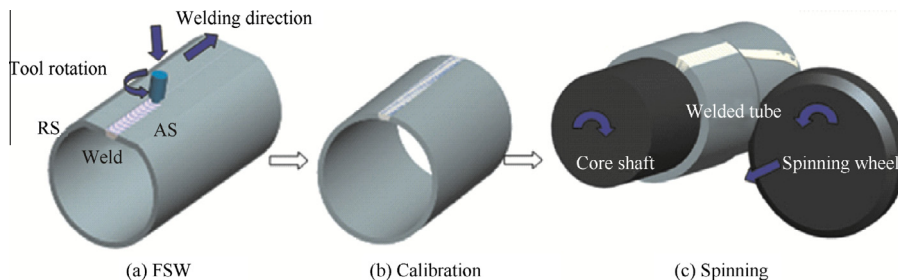

Fig. 6   Schematic of tube welding and spinning process.[76]

thinning and fracture. He found that the weld significantly reduced the forming limit of the welded tube when the weld was located on the outside, while the weld showed an almost negligible effect on the forming limit when the weld was located on the inside or near the neutral layer; the boost at the back of the tube or fewer balls could improve the forming limit of the welded tube. Based on these analyses, the qualified bent QSTE340 welded tubes with the small bending radius was successfully obtained by means of NC bending.

4.3. Existing problems and development directions

In recent years, many researchers have shown that the position and time of occurrence of the bending fracture of the uniform tubes can be predicted accurately by combining appropriate ductile fracture criterion with the FEM.[3,79,80] A ductile fracture criterion contains at least one or two damage constants; therefore, at least one or two destructive tests, such as a uniaxial tensile test and a plane tensile test, are required to determine these constants and, thus, the criterion. However, compared with homogeneous tubes, the welded tubes consist of the weld, the HAZ and the parent metal, which have different material properties and widths, even different thicknesses. In addition, the width of the weld is narrow, for example, the width of laser-welded tubes is only 0.4–1.0 mm.[81] Therefore, it is very difficult to obtain the damage constants of the weld and the HAZ accurately. This increases the difficulty in predicting the occurrence of a fracture in the welded tube plastic forming process by using a ductile fracture criterion. As a result, with the wide application of welded tube plastic forming technology in aviation, aerospace, automobile and other fields, research on the forming limit based on other defects, such as wrinkling, other plastic forming processes such as spinning and flaring, and predicting the fracture location and occurrence time of welded tube plastic forming using an appropriate ductile fracture criterion combined with FEM are the key issues that need to be solved in the future.

Much research on welded tubes[13,14,28,58,61] and the tailor-welded plate[82] with the same thickness and the same materials shows that the weld has a significant influence on tailor-welded plate forming due to the constraining effect on the deformation of the HAZ and the parent metal of the welding seam as a quasi-rigid boundary or a rigid inclusion relative to the parent metal. For tailor-welded tubes with different materials and thicknesses, this constraining effect will be more significant. Therefore, research on the deformation behavior and constraining effect of tailor welded tubes with different materials and thicknesses will become one of the trends in the research of welded tube forming.

Until now, almost all the research on the forming limit of welded tubes has been performed from a macro point of view. The macro-scale forming limit model characterizes the instability and failure of the material through macroscopic parameters. The micro-scale forming limit model characterizes the failure of the material using microscopic parameters, such as voids and micro cracks, and the formation, growth and expansion of the void and the micro cracks are the causes of the failure of the material.[83] Much similar research shows that the forming limit curve of blanks predicted by the micro-scale model (such as the anisotropic GTN model) is in better agreement with the experimental results.[84,85] Therefore, characterizing the failure of the material from the micro-scale is a direction for studying the forming limit of welded tubes.

5. Trends and challenges of welded tubes plastic forming

In response to the urgent demands for accurate and efficient manufacturing of high-performance and lightweight welded tubes in the aviation, aerospace and automotive industries, the trends in welded tube plastic forming theories and technologies are shown as follows.

(1) Laser welding has high quality, high flexibility and numerous other advantages. It can not only produce high-quality tubes with large ratios of diameter to thickness but also adopt the combinations of different materials and different thicknesses in different parts according to varying demand. Therefore, with the urgent need for high strength lightweight tubes in the aviation, aerospace and automotive industries, wider use of laser welded high strength steel tube will be a trend.

(2) At present, the application and research of plastic forming of welded tubes are concentrated on bending, hydroforming and spinning processes. Because tube-end forming technology, such as flaring and flanging, is an essential process for tube application, welded tube end forming technology will expand its application in the aviation, aerospace and automotive fields in the future.

Regarding the above trends in plastic forming of welded tubes, the challenges needing to be urgently solved are summarized as below.

(1) Compared to welded tubes, research on the inhomogeneous deformation and coordination mechanism of plastic forming of tailor-welded tubes become more important and difficult because they are composed of different materials and thicknesses. However, at present, most of the research focuses on the tailor-welded blanks, while research on tailor-welded tubes is rare. With the extensive application of laser tailor-welding of high strength tubes in the aviation, aerospace and automotive industries, there is an urgent need to carry out research on the inhomogeneous deformation and coordination mechanism of plastic forming of tailor-welded tubes with different materials and thicknesses.

(2) With the plastic forming process of welded tubes expanding from the bending, hydroforming and spinning toward tube-end forming, such as flaring and flanging forming, it is important to perform research on the inhomogeneous deformation and coordination mechanism of welded tube-end forming.

(3) To accurately simulate plastic forming processes of welded tubes, the FE modeling considering effects of welding on not only property difference but also residual stresses as well as welding distortions and microstructure is needed. For this purpose, how to establish the modeling for the complete process chain including thermo-mechanical coupled welding, heat treating, followed by the particular plastic forming could be a challenge.

(4) The research characterizing the forming limit of welded tubes is only focused on the fracture forming limit of welded tubes in hydroforming and bending processes from the macro point of view, and no general ductile fracture criterion has been established. To accurately predict the fracture forming limit, a general ductile fracture criterion that considers the material characteristics of welded tubes is needed. Considering that other defects in addition to fracture, e.g., wrinkling, usually occur easily in the plastic forming process of welded tubes, research on the forming limit of other defects is needed. Because the fracture failure of the material has a close relationship with the voids and micro cracks, to analyze the fracture mechanism, it is necessary to perform researches on the forming limit of welded tubes from the micro point of view.

macro or micro ductile fracture criterion considering the material characteristics of welded tubes, and of other defects.

6. Conclusions

(1) Welded tube plastic forming responds to the current urgent demands for high-performance and lightweight components and accurate, short-cycle, low-cost manufacturing technology in high-tech industries such as aviation, aerospace and automobiles. The current urgent demand for high efficiency and precision production are integrally related to the constraint effect of the weld zone on the plastic forming of welded tubes and to the inhomogeneous deformation and coordination mechanism in welded tube plastic forming. This depends on the insight into the nonlinearity of materials, geometrical effects, the complicated contact conditions and the boundary conditions of the welded tubes, and the coupling effect among them. Thus, advances in the studies of these common topics in welded tube plastic forming are summarized, including material properties and modeling of welded tubes, weld characterization in FE modeling, constraining effect and deformation coordination in welded tube plastic forming, and the forming limit of welded tubes.

(2) With the increasing demand for better performance tubes, more complex welded tubular components with lighter-weight materials are required. These components are characterized by their thin wall thickness, large diameter, and the combination of different materials and thicknesses. The tubular materials are generally hard to deform, with limited ductility and high strength. Considering the facts of tough tolerances in applications and multiple constraints with nonlinear contact conditions in plastic forming, several challenges need to be overcome, namely, the FE modeling for the complete process chain including tube welding, heat treating and plastic forming process of welded tubes; the inhomogeneous deformation and coordination mechanism of plastic forming of tailor-welded-tubes with different materials and thicknesses; the inhomogeneous deformation and coordination mechanism of welded tube-end forming; more comprehensive research on the forming limit of welded tubes, from the point of view of the

References

1. Koc M, Altan T. An overall review of the tube hydroforming (THF) technology. *J Mater Process Technol* 2001;**108**(3):384–93.
2. Kleiner M, Homberg W, Brosius A. Process and control of sheet metal hydroforming. *Proceedings of the 6th ICTP*; 1999 Sep 19–24; Nuremberg, German. Berlin: Springer; 1999.
3. Kim J, Kim YW, Kang BS, Hwang SM. Finite element analysis for bursting failure prediction in bulge forming of a seamed tube. *Finite Elem Anal Des* 2004;**40**(9–10):953–66.
4. Zhao BY, Wang XS, Ding FC, Miao QB. Hydroforming of compensator joints in rocket's boost transport system. *Aerosp Mater Technol* 2006;**36**(6):52–5 [Chinese].
5. Chen SJ. Microstructure evolution and mechanical behavior of heterogeneous joint and plastic deformation optimization of SUS304 tailor-welded tube [dissertation]. Harbin: Harbin Institute of Technology, 2012 [Chinese].
6. Khalfallah A. Experimental and numerical assessment of mechanical properties of welded tubes for hydroforming. *Mater Des* 2013;**56**(4):782–90.
7. Ghoo BY, Keum YT, Kim YS. Evaluation of the mechanical properties of welded metal in tailored steel sheet welded by CO_2 laser. *J Mater Process Technol* 2001;**113**(1–3):692–8.
8. Panda SK, Ravi KD, Kumar H, Nath AK. Characterization of tensile properties of tailor welded IF steel sheets and their formability in stretch forming. *J Mater Process Technol* 2007;**183**(2–3):321–32.
9. Yang TB, Yu ZQ, Xu CB, Li SH. Numerical analysis for forming limit of welded tube in hydroforming. *J Shanghai Jiaotong Univ* 2011;**45**(1):6–10 [Chinese].
10. Bi HY, Lu MH. Weld shape evaluation and metallographic examination of ERW pipes. Baosteel Technology 2006;(3):23–6 [Chinese].
11. Loukus A, Subhash G, Imaninejad M. Mechanical properties and microstructural characterization of extrusion welds in AA6082-T4. *J Mater Sci* 2004;**39**(21):6561–9.
12. Ren N, Zhan M, Yang H, Qin YT, Zhang ZY, Jiang HM, et al. Weld characteristic and NC bending formability study of QSTE340 welded tube. *Trans Tianjin Univ* 2011;**17**(4):288–92.
13. Li Y, Zhan M, Wang JG, Ren N, Yang H. FE analysis of NC bending of thin-walled CP3 welded tubes. Aeronautical Manufacturing Technology 2011;(16):86–93 [Chinese].
14. Ren N. Study on deformation compatibility and bending limit in steel welded tube NC bending processes [dissertation]. Xi'an: Northwestern Ploytechnical University, 2013 [Chinese].
15. Chan LC, Chan SM, Cheng CH, Lee TC. Formability and weld zone analysis of tailor-welded blanks for various thickness ratios. *J Eng Mater Technol* 2005;**127**(2):179–85.

16. Kim HJ, Heo YM, Kim N, Seo D. Forming and drawing characteristics of tailor welded sheets in a circular draw bead. *J Mater Process Technol* 2000;**105**(3):294–301.

17. Min KB, Kim KS, Kang SS. A study on resistance welding in steel sheets using a tailor-welded blank (1st report): Evaluation of upset weldability and formability. *J Mater Process Technol* 2000;**101**(1–3):186–92.

18. Chung K, Lee W, Kim D, Kim J, Chung KH, Kim C, et al. Macro-performance evaluation of friction stir welded automotive tailor-welded blank sheets: part I-Material properties. *Int J Solids Struct* 2010;**47**(7–8):1048–62.

19. Cheng CH, Jie M, Chan LC, Chow CL. True stress–strain analysis on weldment of heterogeneous tailor-welded blanks–a novel approach for forming simulation. *Int J Mech Sci* 2007;**49**(2):217–29.

20. Zhan M, Du HF, Liu J, Ren N, Yang H, Jiang H, et al. A method for establishing the plastic constitutive relationship of the weld bead and heat-affected zone of welded tubes based on the rule of mixtures and a microhardness test. *Mater Sci Eng A* 2010;**527**(12):2864–74.

21. Milian JL, Adonyi Y. Formability of tailored blanks for automotive applications. *34th MWSP conference proceedings*; Montreal, Canada. ISS-AIME; 1992.p. 83–91.

22. Stasik MC, Wagoner RH. Forming of tailor-welded aluminum blanks. *Int J Form Process* 1998;**1**:9–34.

23. Davies RW, Smith MT, Khaleel MA, Pitman SG, Oliver HE. Weld metal ductility in aluminum tailor welded blanks. *Metall Mater Trans A* 2000;**31**(11):2755–63.

24. Reis A, Teixeira P, Duarte JF, Santos A, Rocha ABD, Fernandes AA. Tailored welded blanks-an experimental and numerical study in sheet metal forming on the effect of welding. *Comput Struct* 2004;**82**(17):1435–42.

25. Abdullah K, Wild PM, Jeswiet JJ, Ghasempoor A. Tensile testing for weld deformation properties in similar gage tailor welded blanks using the rule of mixtures. *J Mater Process Technol* 2001;**112**(1):91–7.

26. Lee W, Chung K, Kim D, Kim J, Kim C, Okamoto K, et al. Experimental and numerical study on formability of friction stir welded TWB sheets based on hemispherical dome stretch tests. *Int J Plast* 2009;**25**(9):1626–54.

27. Kim D, Lee W, Kim J, Kim C, Chung KD. Formability evaluation of friction stir welded 6111–T4 sheet with respect to joining material direction. *Int J Mech Sci* 2010;**52**(4):612–25.

28. Ren N, Zhan M, Yang H, Zhang ZY, Qin YT, Jiang HM, et al. Constraining effects of weld and heat-affected zone on deformation behaviors of welded tubes in numerical control bending process. *J Mater Process Technol* 2012;**212**(5):1106–15.

29. Reynolds AP, Duvall F. Digital image correlation for determination of weld and base metal constitutive behavior. *Weld J* 1999;**78**(10):S355–60.

30. Brauser S, Pepke LA, Weber G, Rethmeier M. Deformation behavior of spot-welded high strength steels for automotive applications. *Mater Sci Eng A* 2010;**527**(26):7099–108.

31. Tung SH, Shih MH, Kuo JC. Application of digital image correlation for anisotropic plastic deformation during tension testing. *Opt Lasers Eng* 2010;**48**(5):636–41.

32. Genevois C, Deschamps A, Vacher P. Comparative study on local and global mechanical properties of 2024 T351, 2024 T6 and 5251 O friction stir welds. *Mater Sci Eng A* 2006;**415**(1–2):162–70.

33. Hatamleh O. Effects of peening on mechanical properties in friction stir welded 2195 aluminum alloy joints. *Mater Sci Eng A* 2008;**492**(1–2):168–76.

34. Brown R, Tang W, Reynolds AP. Multi-pass friction stir welding in alloy 7050–T7451: effects on weld response variables and on weld properties. *Mater Sci Eng A* 2009;**513–514**:115–21.

35. Leitão C, Galvão I, Leal RM, Rodrigues DM. Determination of local constitutive properties of aluminium friction stir welds using digital image correlation. *Mater Des* 2012;**33**:69–74.

36. Zadpoor AA, Sinke J, Benedictus R. Finite element modeling and failure prediction of friction stir welded blanks. *Mater Des* 2009;**30**(5):1423–34.

37. Zadpoor AA, Sinke J, Benedictus R. Global and local mechanical properties and microstructure of friction stir welds with dissimilar materials and/or thicknesses. *Metall Mater Trans A* 2010;**41**(13):3365–78.

38. Boyce B, Reu P, Robino C. The constitutive behavior of laser welds in 304L stainless steel determined by digital image correlation. *Metall Mater Trans A* 2006;**37**(8):2481–92.

39. Scintilla LD, Tricarico L, Brandizzi M, Satriano AA. Nd:YAG laser weld ability and mechanical properties of AZ31 magnesium alloy butt joints. *J Mater Process Technol* 2010;**210**(15):2206–14.

40. Louëdec GL, Pierron F, Sutton MA, Reynolds AP. Identification of the local elasto-plastic behavior of FSW welds using the virtual fields method. *Exp Mech* 2013;**53**(5):849–59.

41. Chao YJ, Sutton MA, Peter WH, Luo PF. Measurement of three-dimensional displacements in deformable bodies by digital image processing. *Spring Conference on Experimental Mechanics*; 1989 May 29-Jun 1; Cambridge MA. Springer; 1989. p. 139–46.

42. Li GY, Xu FX, Sun GY, Li Q. Identification of mechanical properties of the weld line by combining 3D digital image correlation with inverse modeling procedure. *Int J Adv Manuf Technol* 2014;**74**(5–8):893–905.

43. Dick CP, Korkolis YP. Strength and ductility evaluation of cold-welded seams in aluminum tubes extruded through porthole dies. *Mater Des* 2015;**67**:631–6.

44. Fu L, Liu DH, Sun YG, Li GY, Xu FX, Chen SS. A refined method to identify material parameters of weld line based on DIC technique and hardness test. *Chin Mech Eng* 2013;**24**(2):274–9 [Chinese].

45. Chen SS, Lin JP. A novel method for measuring the weld property of tailor welded blanks based on DIC. *Trans Chin Weld Inst* 2013;**34**(8):76–80 [Chinese].

46. Tian HB, Lin JP, Liu RT, Xun YC. A review on ultralight auto body and related forming technologies. *Automot Eng* 2005;**27**(3):381–4 [Chinese].

47. Bhagwan AV, Kridli GT, Friedman PA. Influence of weld characteristics on numerically predicted deformation behavior of aluminum tailor welded blanks. SAE Technical Paper; 2002. No.: 2002-01-0386.

48. Zhao KM, Chun BK, Lee JK. Finite element analysis of tailor-welded blanks. *Finite Elem Anal Des* 2001;**37**(2):117–30.

49. Meinders T, Berg AVD, Huétink J. Deep drawing simulations of tailored blanks and experimental verification. *J Mater Process Technol* 2000;**103**(1):65–73.

50. Zimniak Z, Piela A. Finite element analysis of a tailored blanks stamping process. *J Mater Process Technol* 2000;**106**(1–3):254–60.

51. Iwata N, Matsui M, Nakagawa N, Ikura S. Improvements in finite-element simulation for stamping and application to the forming of laser-welded blanks. *J Mater Process Technol* 1995;**50**(1–4):335–47.

52. Jiang H, Li SH, Wu H, Chen XP. Numerical simulation and experimental verification in the use of tailor-welded blanks in the multi-stage stamping process. *J Mater Process Technol* 2004;**151**(1–3):316–20.

53. Nakagawa N, Ikura S, Natsumi F, Iwata N. Finite element simulation of stamping a laser-welded blank. SAE Technical Paper; 1993. No.: 930522.

54. Kampuša Z, Balič J. Deep drawing of tailored blanks without a blank holder. *J Mater Process Technol* 2003;**133**(1–2):128–33.

55. Raymond SD, Wild PM, Bayley CJ. On modeling of the weld line in finite element analyses of tailor-welded blank forming operations. *J Mater Process Technol* 2004;**147**(1):28–37.

56. Galdos L, Garcia C. Innovative method for welded tube characterization and tube hydroforming process modeling. *Proceedings of the 8th ICTP: Advanced Technology of Plasticity*; 2005 Oct 9–13; Verona, Italy. Springer; 2005.p. 299–307.

57. Rogue AP, Natal Jorge RM, Parente MPL, Valente RAF, Fernandes AA. Influence of the heat affected zone on hydroforming with tailor-welded tubular blanks. In: Oñate E, Owen DRJ, editors. *International Conference on Computational Plasticity*; 2005.p.1-4.

58. Liu J, Yang H, Zhan M, Ren N. Finite element modeling of seamed tube NC bending process and its application. *Mater Res Innov* 2011;**15**(s1):s315–8.

59. Chu GN, Wang XS. Laser weld-seam modeling for finite element analysis during tailor-welded tube hydroforming. *J Mech Eng* 2012;**48**(22):34–9 [Chinese].

60. Lee CH, Baek JH, Chang KH. Bending capacity of girth-welded circular steel tubes. *J Constr Steel Res* 2012;**75**:142–51.

61. Lacki P, Adamus K, Wieczorek P. Theoretical and experimental analysis of thermo-mechanical phenomena during electron beam welding process. *Comput Mater Sci* 2014;**94**:17–26.

62. Xu S, Wang W, Chang Y. Using FEM to predict residual stresses in girth welding joint of layered cylindrical vessels. *Int J Press Vessels Pip* 2014;**119**:1–7.

63. Xu S, Zhao Y. Using FEM to determine the thermo-mechanical stress in tube to tube-sheet joint for the SCC failure analysis. *Eng Fail Anal* 2013;**34**:24–34.

64. Yang H, Li H, Zhang Z, Zhan M, Liu J, Li GJ. Advances and trends on tube bending forming technologies. *Chin J Aeronaut* 2012;**25**(1):1–12.

65. Liu J, Yang H, Zhan M, Ren N, Jiang HM, Diao KS, et al. Influence of weld relative strength on wrinkling and wall thickness distribution of thin-walled seamed tube in rotary draw bending process. *Mater Sci Technol* 2011;**19**(6):1–6 [Chinese].

66. Aue-U-Lan Y, Ngaile G, Altan T. Optimizing tube hydroforming using process simulation and experimental verification. *J Mater Process Technol* 2004;**146**(1):137–43.

67. Sun KR, Yang LF. Tailor-welded tube in hydroforming and influence of the heat affected zone on bulge forming. *J Guilin Univ Electron Technol* 2006;**26**(5):380–4 [Chinese].

68. Sun KR, Yang LF. Comparison of deformation behaviors of seamed tube and seamless tubes in hydroforming. *Chin Mech Eng* 2006;**17**(Suppl.):27–31 [Chinese].

69. Liu G, Chu GN, Yu C, Yuan SJ. Deformation compatibility of hydroforming for tailor-welded tube with dissimilar thickness. *J Basis Sci Eng* 2009;**17**(3):477–84 [Chinese].

70. Chu GN, Liu G, Yuan SJ. Plastic deformation regularity of tailor-welded tube (twt) with dissimilar thickness during hydro-bulging. *Acta Metall Sinica* 2008;**44**(12):1479–84 [Chinese].

71. Chu GN, Liu G, Yuan SJ, Liu WJ. Weld seam movement of tailor-welded tube during hydrobulging with dissimilar thickness. *Int J Adv Manuf Technol* 2012;**60**(9):1255–60.

72. Imaninejad M, Subhash G, Loukus A. Influence of end-conditions during tube hydroforming of aluminum extrusions. *Int J Mech Sci* 2004;**46**(8):1195–212.

73. Yuan SJ, Hu ZL, Wang XS. Formability and microstructural stability of friction stir welded Al alloy tube during subsequent spinning and post weld heat treatment. *Mater Sci Eng A* 2012;**558**:586–91.

74. Wang XS, Hu ZL, Yuan SJ, Hua L. Influence of tube spinning on formability of friction stir welded aluminum alloy tubes for hydroforming application. *Mater Sci Eng A* 2014;**607**:245–52.

75. Zhang HL, He J, Li XH, Deng R. Effect of deeply cold spinning on properties of ultra-thin-wall large radius-thickness ratio nickel-based alloy welded cylinder. *Mater Mech Eng* 2011;**35**(6):68–71 [Chinese].

76. Yuan SJ, Hu ZL, Wang XS. Evaluation of formability and material characteristics of aluminum alloy friction stir welded tube produced by a novel process. *Mater Sci Eng A* 2012;**543**(5):210–6.

77. Ma CH, Yu ZQ, Chen XP, Chen XF, Lin ZQ. Experimental study on forming limit diagram of laser welded tube hydroforming. *J Mech Eng* 2013;**49**(2):49–53 [Chinese].

78. Chen XF, Yu ZQ, Hou B, Li SH, Lin ZQ. Prediction model for forming limit of welded tube hydroforming. *J Mech Eng* 2011;**47**(20):116–20 [Chinese].

79. Li H, Yang H, Zhan M. A study on critical thinning in thin-walled tube bending of al-alloy 5052O via coupled ductile fracture criteria. In: Barlat F, Moon YH, Lee MG, editors. *Proceedings of the 10th International Conference*; 2010 Jun 13–17; Pohang, Korea. AIP Publishing; 2010. p. 1286–94.

80. Zhan M, Gu CG, Jiang Z, Hu L, Yang H. Application of ductile fracture criteria in spin-forming and tube-bending processes. *Comput Mater Sci* 2009;**47**(2):353–65.

81. Anand D, Boudreau G, Andreychuk P, Chen DL, Bhole SD. Forming behaviour of tailor (laser)-welded blanks of automotive steel sheet. *Can Metall Q* 2006;**45**(2):189–98.

82. Saunders FI, Wagoner RH. Forming of tailor-welded blanks. *Metall Mater Trans A* 1996;**27**(9):2605–16.

83. Li YH, Lin JP. Status-quo and trends of researches on tailor welded blanks for vehicle body. *Automot Eng* 2014;**36**(6):763–7 [Chinese].

84. Abbasi M, Bagheri B, Ketabchi M, Haghshenas DF. Application of response surface methodology to drive GTN model parameters and determine the FLD of tailor welded blank. *Comput Mater Sci* 2012;**53**(1):368–76.

85. Kami A, Dariani BM, Vanini AS, Dan SC, Banabic D. Numerical determination of the forming limit curves of anisotropic sheet metals using GTN damage model. *J Mater Process Technol* 2015;**216**:472–83.

Zhan Mei is a professor and Ph.D. supervisor at School of Materials Science and Engineering, Northwestern Polytechnical University, Xi'an, China. She received the Ph.D. degree from the same university in 2000. Her current research interests are the unequal deformation theory and precision plastic forming technology of thin-walled complex components of hard-to-deform materials, including bending forming of tubes, spinning of complicates, and electromagnetic forming of intefral airframe structures.

Guo Kun is a M.D. student at School of Materials Science and Engineering, Northwestern Polytechnical University. She received her B.S. degree from Northeastern University in 2014. Her area of research includes bending forming of tubes and electromagnetic forming of integral panel.

Yang He is a professor and Ph.D. supervisor at School of Materials Science and Engineering, Northwestern Polytechnical University, Xi'an, China. He received the Ph.D. degree from the Harbin Institute of Technology in 1990. His current research interests are precise plastic forming about aluminum alloy, magnesium alloy and titanium alloy, high performance lightweight forming of complex structures, and inhomogeneous deformation of difficult to deform materials.